Machine Learning Approach for MRI Brain Tumor Detection using Regularized Extreme Learning

1st R. K. Agrawal
Department of Electronics and Telecommunication Engineering
SNJB's K B Jain College of Engineering
Chandwad, India
agrawal.rkcoe@snjb.org

2nd Mohammad Shabbir Alam
Department of Computer Science
College of Engineering & Computer Science, Jazan University
Jizan, Kingdom of Saudi Arabia
amushabbir@gmail.com

3rd Rajesh Kumar A
Department of Artificial Intelligence and Data Science
N.S.N. College of Engineering and Technology
Karur, India
arurajesh1980@gmail.com

4th N. Aparna
Department of Electronics and Communication Engineering
Hindusthan College of Engineering and Technology
Coimbatore, India
aparnaganesen@gmail.com

5th Gayathri Devi S
Department of Computer Science and Engineering
Vels Institute of Science, Technology & Advanced Studies (VISTAS)
Chennai, India
gayathri.s7@gmail.com

6th Amit Jain
Department of Computer Science and Engineering
Guru Nanak Dev Engineering College
Ludhiana, India
amitjaincse@gndec.ac.in

2025 3rd International Conference on Data Science and Information System (ICDSIS) | 979-8-3315-4265-8/25/$31.00 ©2025 IEEE | DOI: 10.1109/ICDSIS65355.2025.11070823

***Abstract*—One of the most useful imaging methods for finding brain tumors is magnetic resonance imaging. Among the deadliest human diseases, brain tumors rank high. Brain MRI is a lifesaver for radiologists when it comes to diagnosing and treating patients with brain tumors. Radiologist have utilized magnetic resonance imaging (MRI), a relatively new imaging method, to visualize the anatomy and physiology of the human body. Whether a tumor is benign or malignant, it can be utilized to characterize it and track its course. The output weights may be efficiently derived using the suggested GELM model, which shares a closed form solution with the classic DCN, RCNN, UNet. The numerical results show that the suggested method is effective in identifying abnormal and normal tissue from brain MRI images with a higher level of accuracy (94.54%), sensitivity (93.34%), and specificity (93.47%).**

Keywords—brain tumor detection (BTD), magnetic resonance imaging (MRI), potential field segmentation (PFS), graph regularized extreme learning machine (GELM), densely connected networks (DCN).

I. INTRODUCTION

The brain is the seat of executive function in a human being. Over an extensive system of connections and neurons, it is in charge of carrying out all operations. An aberrant proliferation of brain cells that impacts neurological system functions is the cause of a brain tumor, one of the most dangerous disorders [1]. A physician's expertise and knowledge are crucial in the crucial step of brain cancer classification. To aid radiologists and doctors in the detection of brain tumors, an automated tumor classification system is crucial. A brain tumor in a human being is the result of unchecked cell growth. There are two categories: malignant and benign. A malignant tumor contains cancerous cells, whereas a benign tumor is a homogeneous structure free of them. According to the American Brain Tumor Association and the World Health Organization (WHO), a tumor grading system has been established, with grades I and II being referred to as benign, and grades III and IV as malignant [2]. When contrasted with malignant growth, benign growth is much slower. Using any radiation from ions, Magnetic resonance imaging (MRI) provides a precise picture of the human brain's anatomy. Although this technique works well for segmenting brain tumors, it struggles to identify normal and unhealthy areas in a single MRI. The brain's activity and even healthy cells can be negatively impacted by unchecked cell development. With the advancement of technology; imaging techniques have contributed to the study of the structure and function of the brain. MRI can pinpoint the exact location of a tumor. But in order to treat a tumor, radiologists must first determine its size [3]. When it comes to diagnosing and treating tumors with machine learning, image processing approaches are crucial for the monitoring of tumor sites between computers and doctors. Brain tumor MR image recognition and self- classification made use of a wide variety of techniques. Conventional wisdom holds that CT and MRI scans are the gold standard for diagnosing brain tumors.

MRI in particular provides high-quality images owing to its sophisticated magnetic technology, illuminating the brain's structure in great detail. If a tumor is suspected to be located in the brain or spinal cord, an MRI of that area will be chosen. These imaging techniques have their uses, but they also have their limitations. Diagnostic mistakes may occur due to the subjectivity of picture interpretation, which can compromise the precision of tumor characterization [4]. In addition, a definitive diagnosis may require a battery of testing, which can add both time and money to the procedure. It is challenging to diagnose brain tumors due to the intricate brain structure that results from the interconnected nature of all brain tissues. Segmentation has gained a lot of attention and popularity in treatment monitoring and surgery planning, even if classification approaches are also important. A major reason for this is a development in image guided surgery. Necrosis, edema, and the active tumorous core are some of the tumor structures that will primarily be delineated throughout this segmentation phase. The segmentation techniques that are now available can be categorized as either edge-based or region-based. The methodology utilized to select and analyze relevant publications will be thoroughly discussed, with an emphasis on the analysis criteria and procedures that were used to obtain useful insights. Surgery, radiation treatment, and chemotherapy are common forms of treatment, with specific regimens adapted for each patient based on age, general health, tumor type, and location.

Radiation therapy attempts to shrink the tumor while surgery attempts to eradicate it entirely. Radiation treatment and chemotherapy seek for and kill tumor cells, whereas surgery attempts to remove the tumor in its entirety. Treatment

advances have improved results, but tumor features and early identification determine prognosis [5]. Current research frequently employs conventional statistical or machine learning models in isolation, which may inadequately represent the intricate, nonlinear relationships between logistics performance metrics and economic variables. This work presents a RELM approach to mitigate these constraints. The RELM component manages over dispersed count data and optimizes parameter choices to enhance predictive performance. The goal of this research is to help improve patient outcomes by creating diagnostic tools that are more precise and efficient by investigating the use of artificial intelligence in medical imaging.

Section 2 explains the relevant works. In Section 3, we offer the proposed way and in Section 3, we present the traditional approaches. Section 4 presents and discusses experimental comparisons on an MRI benchmark dataset between the individual segmentation methods and the ensemble approaches. Lastly, Section 5 provides the final observations.

II. Literature Survey

The literature suggests a hybrid method for using MRIs to detect and classify brain tumors. The bounding boxes of bone structures on MRI are identified using a Support Vector Machine (SVM) and non-linear regression [6]. By utilizing local information, such as textural cues, and forming associations between the relative locations of pelvic bone components, the proposed model is able to identify their placements. Novels introduced Convolutional Neural Networks (CNN) [7]. The study's suggested method outperformed the genetic algorithms KNN, SVM, and CNN in terms of accuracy, according to the evaluation results. It suggested using MLBPNN, an approach for brain tumor classification systems that is based on ML [8]. It utilized Extreme Learning Machine (ELM-LRF), an algorithm developed, to classify and detect brain tumors. To begin, in order to ignore noise, non-local measures and local smoothing techniques have been employed. Step two involved classifying cranial MR images as either benign or malignant using ELM-LRF. Image analysis for Brain Tumor diagnosis and feature extraction based on Magnetic Resonance images was initiated by [9] using the Berkeley Wavelet Transform and Support Vector Machine (BWT SVM) [10]. In order to assign a label to the central pixel, the majority of CNN-based algorithms use 2D or 3D patches extracted from MR images.SVM , Fuzzy C-means (FCM) [11] and Decision Forests (DF) are among the most applied discriminative methods. The most accurate brain tumor segmentation algorithm was the Random Forests (RF) algorithm.

Semantic segmentation, scene classification, and tissue categorization are all areas where CNNs have shown effective. A further limitation with these methods is that they tend to over-fit the data, which can be mitigated by using RF [12]. But new findings show that Deep Learning (DL)-based approaches beat standard discriminative models. CNNs are another popular DL method; they do very well with both two- and 3-D medical pictures. We suggested a feature selection method to further reduce computing time and improve efficiency. Afterwards, the ELM was used to categories the robust features that were produced using this technique. A Generative Adversarial Network (GAN)-based approach ELM-based learning residual network standard-features-based classification adaptive independent subspace analysis, transfer learning based tumor classification and Excitation DNN are some of the other methods introduced in the literature for brain tumor classification [13]. On top of that, to gaçaretal. Debugging and issue discovery can be challenging with LSTMs due to their complexity compared to CNNs and RNNs [14]. Furthermore, the significance of transfer learning for DL feature extraction was also explained. As a result, the traditional manual processes must be replaced with automated technologies. Both the previous multimodal BraTS tests and the findings from the last decade show that Deep Neural Networks (DNNs) perform exceptionally well [15].

A lot of focus has been on learning with local consistency of data as a means to enhance the performance of current deep learning models as of late. We propose a discriminative graph regularized Extreme Learning Machine (GELM) in this research based on the premise that related samples should share similar features. Constraints on output weights in GELM ensure that samples within the same class produce consistent results. An analytical solution to the output weights is also achieved by adding the regularization term to the aim of the basic ELM model, which is how the constraint is formulated. In order to assess how well GELM works, we run experiments on four popular face data bases. The experimental results show that GELM outperforms simple ELM and state-of-the-art models in most circumstances.

III. Proposed System

Among the most difficult and time-consuming tasks in medical image processing is the detection and segmentation of brain tumors. Magnetic resonance imaging, or MRI, is a non-invasive medical imaging method that doctors primarily utilize to see the human body's internal structures. It is a challenging process to classify tumors as malignant or benign after proper segmentation of brain MR images because of the complexity and variety in tumor tissue features such shape, size, grey level intensities, and location.

There are four categories in this RAR archived dataset: three for tumors (pituitary, glioma, and meningioma) and one for normal MRI [16] images of the brain. The data cleanliness is the strongest point of this dataset when compared to previous releases on Kaggle. To that end, we ran a thorough data cleaning workflow on the raw dataset. Improving the dataset's integrity and usefulness was the goal of this pipeline's multiple steps.

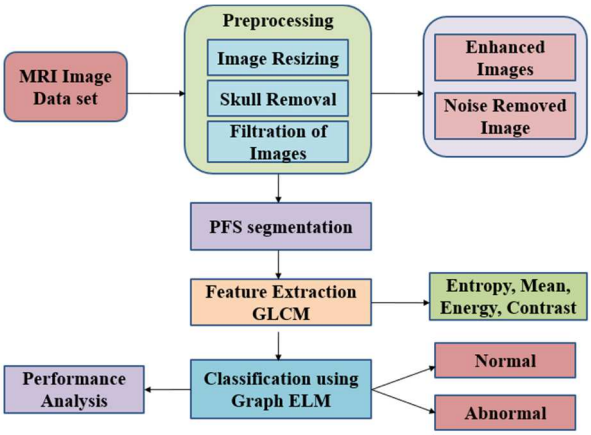

Fig. 1. Block Diagram for Proposed GELM

In Figure 1, we can see the suggested method's development. To begin, MRI data of brain tumors was

acquired and preprocessed to remove noise using ACEA and the median filter.

A. Data Preprocessing

The following are the main operations that will be applied to the MRI pictures in this step to ensure that the system can read the correct input and improve the conditions for image analysis:

1) Image Resize: In this stage, we will establish a fixed size, such as (32 × 32), to examine the entire dataset under the same conditions, taking into account that the input images have varying height and breadth. Skull Removal: This stage involves removing the background and extracting the brain's skull, which is necessary because the brain is so important [17]. The skull surrounding the brain serves several purposes.

2) Filtration of Image: In order to improve the likelihood of feature detection and to make the median filter applicable in both training and testing situations, it is applied to MRI images at this stage.

B. Segmentation

1) Potential Field Segmentation: Following Potential Field Clustering, we expand upon it. A magnetic resonance imaging (MRI) scan is represented by the set of pixels $J = \{O_1, O_2, \dots, O_m\}$where each pixel $p_i \phi \mathbb{Q}^2$ has a corresponding grey intensity value $0 \leq x_j \leq 255$. Identifying the subset $T_{OET} \subset J$ of tumor pixels is the goal. According to the comparison, the charge or mass that generates the potential field is the pixel intensity. Take note that there is a practical limitation on the number of masses (i.e., pixel intensities) that may be used to determine the potential field at a given position in a digital image due to the fact that it is a discretisation. The number of places at which the potential field is calculated must likewise be finite for implementation purposes. Since there are an identical number of pixels in the image, we'll set the number of points equal to that.

There are multiple stages to the segmentation algorithm. Determining the potential field for each pixel p_i is the initial stage [18]. our violates the physical analogy: at one point (another pixel in our example), a potential field originates from the pixels, which have positions in the two-dimensional picture space.

A pixel's potential at location p_i is equal to the sum of all of its individual potentials, where $\Omega_i(p_i)$ is the potential that pixel p_i creates at position p_j as shown in Equation (1).

$$\Omega(p_i) = \sum_{i=1}^{m} \Omega_i(p_i) \quad (1)$$

Equation (2) shows the distinct potential field functions $\Omega_i(p_i)$ can be expressed in a wide variety of mathematical ways. Next, you'll need to determine an adaptive potential threshold.

$$s_\Omega = \Omega_{min} + (\Omega_{max} - \Omega_{min)\alpha} \quad (2)$$

Where the values of the potential fields for each of the $m\Omega(p_i)$ variables range from $0 \leq \alpha \leq 1$, with Ω_{max} and Ω_{min} being the upper and lower bounds, respectively. Every pixel p_i that has a $\Omega(p_i) \leq s\Omega$ is linked to the tumor set T_{OET} in the third phase. Since tumor pixels have a bigger mass, the potential of the surrounding regions is also substantially larger than in other regions with smaller or no mass, making this small potential segmentation criterion intuitively valid. Here is a summary of this segmentation strategy in Algorithm 1.

Algorithm 1: Potential Field Segmentation

Input: $MRI\ J, \alpha$

Output: Segmentation $T_{OET}\ of\ J$

$T_{OET} = \delta, \Omega_{min} = 0, \Omega_{max} = largenumber$
for $each\ p_i \phi J$ do
$\Omega(p_i) = 0$
for $each\ p_j \phi J$ do
$\Omega(p_i) = \Omega(pi) + \Omega_i(p_i)$
end for
end for
for $each\ p_i\ \phi J$ do
if $\Omega(p_i) < \Omega_{min}$then
$\Omega_{min} = \Omega(p_i)$
end if
$if\ \Omega(p_i) > \Omega_{max}\ then$
$\Omega_{max} = \Omega(p_i)$
end if
end for
$s_\Omega = \Omega_{min} + (\Omega_{max} - \Omega_{max})\alpha$
$for\ each\ p_i \phi J\ do$
$if\ \ \Omega(p_i) \leq s_\Omega then$
$T_{OET} = T_{OET} \cup \{p_i\}$
end if
end for

Both PFS and PFC have a time complexity of $P(m^2)$, which is a result of the potential field computation being an $P(m^2)$ process. The potential field at pixel p_i, for all m pixels, equals calculated as the total of the individual potentials generated by all the other pixels. The total time complexity is $P(m^2)$, meaning that for every $m$pixels, there are m computations. The first for loop in Algorithm 1 has an inner for loop, which computes potential fields with an $P(m^2)$ complexity. Everything else in Alg. 1 is $P(m)$ Keep in mind that the accuracy of the produced segmentation is the primary metric for performance in this domain, namely medical image segmentation, despite the fact that OET is a quadratic-time technique.

C. Feature Extraction

In order to extract the image features, this approach uses the GLCM technique. To extract the second-order statistical textural properties from a specific brain image, a statistical method called the co-occurrence matrix is applied. Always make sure that the number of grey levels is equal to the number of rows and columns when using GLCM. To extract the [19] first-order histogram-based characteristics, we apply the following equations. The proposed method involves extracting form, textural, and statistical elements from each cluster and feeding them into the classifier to help it detect tumors in the given MRI picture. Here are the features that were extracted in Equation (3):

$$Entropy = \sum_{w=0}^{nl-1} log\ S_{wz} \quad (3)$$

One way to look at the entropy of a random variable is as a measure of how unpredictable it is. The maximum potential value of the co-occurrence matrix is achieved when all of its components are equal.

$$correlation = \frac{\sum_{w=0}^{nl-1}(w,z)s(w,z)-\rho_j\rho_i}{\pi_j\pi_i} \quad (4)$$

The degree of connection between the reference pixel and its neighbours is ascertained by the correlation metric is explained in Equation (4).

$$Energy = \sum_{w=0}^{nl-1} S_{wz}^2 \quad (5)$$

The product of squared dimensions is defined in terms of energy in Equation (5). This establishes the degree to which the mixture is uniform. Pixels with a high energy value are quite similar to one another.

$$Contrast = \sum_{n=0,w=0}^{nl-1} n^2 S(w,z)^2 \quad (6)$$

As derived in Equation (6), a image's contrast is defined as the brightness disparity between a reference pixel and its adjacent pixels.

$$Mean(\rho) = \sum_{w=0}^{nl-1} w.s(w) \quad (7)$$

The mean is a measure of the average brightness of a picture or material. The variation around the mean describes the intensity range of the readings as indicated by Equations (7)-(9).

$$SD(\pi) = \sqrt{\sum_{w=0}^{nl-1}(w-\rho)^2.s(w)} \quad (8)$$

$$Variance(\pi^2)\sum_{w=0}^{nl-1}(w-\rho).s(w) \quad (9)$$

D. Model Training

It is assumed that there is a dataset consisting of M samples and d classifications. There are Ms samples in the s^{th} class, where $M_1 + M_2 + \cdots + M_d = M$. Here Equation (10) define the neighbouring matrix X in a manner similar to the discriminative analysis:

$$X_{ji} = \begin{cases} 1/M_t & if\ both\ g_j\ and\ g_i\ belong\ to\ the\ s^{th}\ class \\ 0 & otherwise \end{cases} \quad (10)$$

$g_j = \left(h_1(w_j), \ldots, h_l(w_j)\right)^S$ represents the hidden layer for input sample w_j, and $g_i = \left(h_1(w_i), \ldots, h_l(w_i)\right)^S$ represents the hidden layer for input sample w_i. Imagine a diagonal matrix C with the following entries: $C_{jj} = \sum_i X_{ji}$, where are the sums of the columns (or rows, as X is symmetric) of X.We are able to calculate the Laplacian of the graph $K = C - X$.

The output weight matrix α maps two vectors, z_j and z_i, to the values of g_j and g_i, respectively.The following objective function Equation (11) should be minimised based on the assumption that z_j and z_i should be similar when g_j and g_i are from the same class:

$$min\sum_{j,i}\left|\left|z_j - z_i\right|\right|_2^2 X_{ji} = Sq(ZKZ^S) \quad (11)$$

The setting for the $Z = \alpha^S G$ Extreme Learning Machine. We may formulate the goal function of graphregularized extreme learning machine as follows by including the graph regularisation terminus into the conventional ELM model:

$$min_\alpha\left|\left|\alpha^S G - S\right|\right|_2^2 + \gamma_1 Sq(\alpha^S GKG^S\alpha) + \gamma_2\left|\left|\alpha\right|\right|_2^2 \quad (12)$$

In this context, γ_1 and γ_2 are regularisation parameters that help to balance the effects of the graph regularisation term $Sq(\alpha^S GKG^S\alpha)$ and the κ_2-norm regularisation term $\left|\left|\alpha\right|\right|^2$as depicted in Equation (12).

Equation (13) may obtain α by setting the derivative of the objective function E with regard to α as zero, as follows:

Set $E \triangleq \left|\left|\alpha^S G - S\right|\right|_2^2 + \gamma_1 Sq(\alpha^S GKG^S\alpha) + \gamma_2\left|\left|\alpha\right|\right|_2^2$

$$\frac{\partial E}{\partial \alpha} = (2GG^S\alpha - 2GS^S) + 2\gamma_1 GKG^S\alpha + 2\gamma_2\alpha \triangleq 0 \quad (13)$$

Algorithm 2 summarises the algorithm description of our proposed graph regularised Extreme Learning Machine.

Algorithm 2: Graph Regularized Extreme Learning Machine
Input: training set $M = \{(w_j s_j)\|w_j \phi \mathbb{Q}^c, s_j \phi \mathbb{Q}^n, j = 1,2,\ldots,M\}$, Function h for activation, quantity of hidden nodes L and Parameters of Regularisation: γ_1 and γ_2.
Output: Display the Weight matrix α;
Assign input weights x_i and biases at random $a_i, i = 1, \ldots, L$;
Determine the output matrix G of the hidden layer; Determine the Laplacian matrix K ; Determine the output weight matrix α.

Data collected from sampling a probability distribution that has support on or near a submanifold of the ambient space has recently [20] been explored by many academics.

The significance of the local geometrical structure in the dataset is highlighted by the fact that, according to the local consistency assumption, close points (neighbours) should typically have comparable features. By building a closest neighbour graph based on some "distance" measurement, several graph embedding (regularisation) upgraded models were proposed, based on local consistency.

IV. Result and Discussion

Many of the body's regulatory processes—including memory, emotions, vision, motor abilities, reactions, and breathing—are controlled by the brain, which is why it is considered one of the most important organs.

The model was evaluated using the publicly available Kaggle dataset, which comprises 3D MRI scans with labelled tumor areas. Performance was assessed by accuracy, sensitivity, specificity, and ROC-AUC.

The RELM model's exceptional sensitivity (93.34%) underscores its capacity for early tumor detection, aiding radiologists in minimizing diagnostic inaccuracies and enhancing patient outcomes.

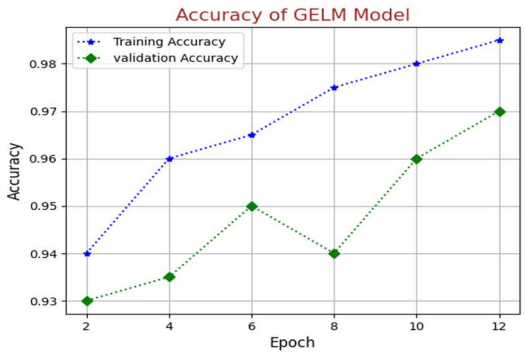

Fig. 2. Accuracy of proposed GELM

Figure 2 shows the results of our model's validation and training runs. A function called keras callbacks computed it. We tested the training and validation accuracy with varying epoch counts.

Table I shows how the model suggested in this study stacks up against others that have used deep learning (DL) techniques to identify brain tumours. A comparative performance assessment reveals that the RELM model substantially exceeds baseline techniques on Acc, Sensitivity, recall and specificity.

This enhancement is ascribed to the model's capacity to handle overdispersed data and refine feature interaction.

TABLE I. PERFORMANCE EVALUTION

Models	Acc	Prec	Recall	F1-Score	Sensitivity	Specificity
DCN	90.61	88.52	86.49	90.65	91.15	91.00
RCNN	89.70	87.63	85.30	89.75	90.27	90.31
GELM	94.54	91.25	89.37	94.60	93.34	93.47
UNet	88.40	86.35	84.39	88.45	92.20	92.48

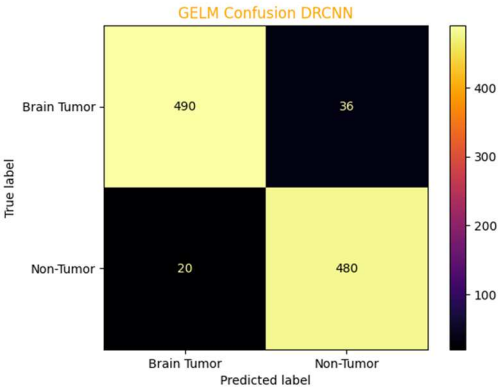

Fig. 3. GELM Confusion Matrix

The GELM in the suggested model identified 490 MRI scans as brain tumors, as shown in Figure 3, while misidentifying 20 scans.

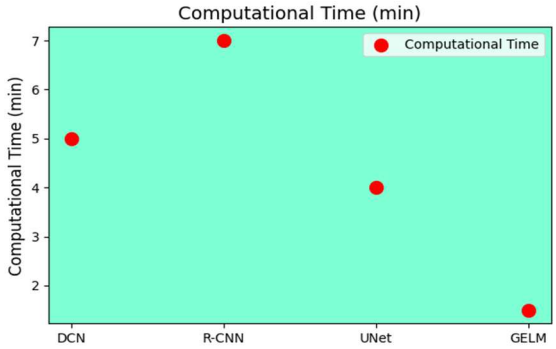

Fig. 4. Comparison of Computational time

Figure 4 provides a comparison of the amount of time required to compute using the recommended strategy with the time required by the standard methods.

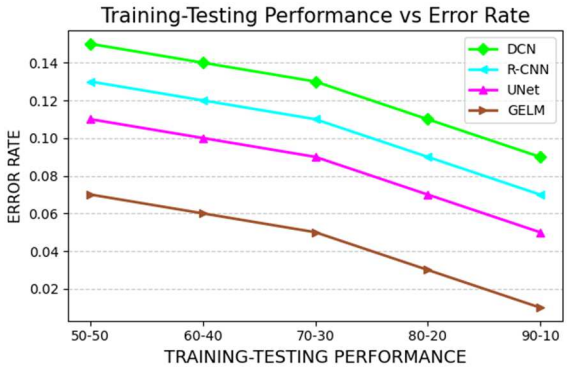

Fig. 5. Error Rate Vs Training-Testing Performace for Brain Tumor

Figure 5 displays the dataset's most inaccurate DCN model. If you want your DCN model to perform better, try using the RCNN, UNET model. The GELM model that was proposed is more accurate than the DCN model.

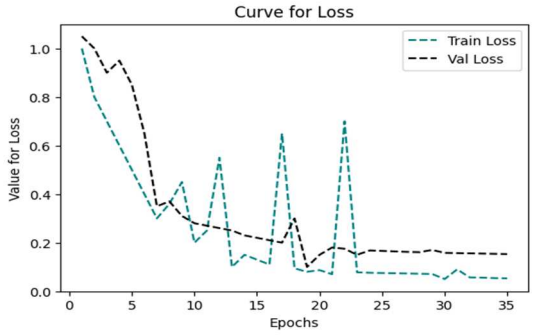

Fig. 6. Training and Validation Loss Value

After the 20th epoch, the loss value approaches zero for both the training and validation sets, and it starts dropping is shown in Figure 6.

V. Conclusion

Since unreliable predictions and diagnoses can emerge from human-assisted manual categorization, brain tumor segmentation ranks high among the challenging but essential challenges in the realm of medical image processing. When compared to DCN, R-CNN, UNet, and other state-of-the-art classification approaches, our experimental results show that our suggested GELM model performs exceptionally well in face recognition. Out of all the models tested, the hybrid model performed the best with GELM at 95.54% and UNET at 88.40%, while DCN and CNN each earned 90.61% and 89.70%, respectively. This study illustrates that RELM offers an effective and precise method for classifying brain tumours utilising MRI images. Its lightweight characteristics and superior performance render it appropriate for use in resource-limited clinical settings. Future endeavours involve the integration of the RELM framework with convolutional autoencoders to improve feature extraction and the expansion of the model to accommodate multi-modal imaging data.

References

[1] A. Gumaei, M. M. Hassan, M. R. Hassan, A. Alelaiwi, and G. Fortino, "A Hybrid Feature Extraction Method With Regularized Extreme Learning Machine for Brain Tumor Classification," IEEE Access, vol. 7, pp. 36266–36273, 2019, doi: 10.1109/ACCESS.2019.2904145.

[2] M. Sharif, J. Amin, M. Raza, M. A. Anjum, H. Afzal, and S. A. Shad, "Brain tumor detection based on extreme learning," Neural Comput. Appl., vol. 32, no. 20, pp. 15975–15987, Oct. 2020, doi: 10.1007/s00521-019-04679-8.

[3] S. Ali Amin, M. K. S. Alqudah, S. Ateeq Almutairi, R. Almajed, M. Rustom Al Nasar, and H. Ali Alkhazaleh, "Optimal extreme learning machine for diagnosing brain tumor based on modified sailfish optimizer," Heliyon, vol. 10, no. 14, p. e34050, Jul. 2024, doi: 10.1016/j.heliyon.2024.e34050.

[4] H. Alsaif, R. Guesmi, B. M. Alshammari, T. Hamrouni, T. Guesmi, A. Alzamil, and L. Belguesmi, "A Novel Data Augmentation-Based Brain Tumor Detection Using Convolutional Neural Network," Appl. Sci., vol. 12, no. 8, p. 3773, Apr. 2022, doi: 10.3390/app12083773.

[5] L. Ma and F. Zhang, "End-to-end predictive intelligence diagnosis in brain tumor using lightweight neural network," Appl. Soft Comput., vol. 111, p. 107666, Nov. 2021, doi: 0.1016/j.asoc.2021.107666.

[6] A. R. Arunarani, V. Bhenia, T. Abirami, N. Aparna, M. Abul Ala Walid, and K. A. Sharada, "An Improved Cuttlefish Optimization Algorithm Based Faster R-CNN for Brain Tumor Detection," Proc. 4th Int. Conf. Smart Electron. Commun. ICOSEC 2023, pp. 1336–1341, 2023, doi: 10.1109/ICOSEC58147.2023.10276261.

[7] R. Saranya, "Image Analysis of MRI - based Brain Tumor Classification and Segmentation using BSA and RELM Networks," 2023 2nd Int. Conf. Autom. Comput. Renew. Syst., pp. 523–528, 2023, doi: 10.1109/ICACRS58579.2023.10405052.

[8] V. Balaji, T. S. Karthik, N. Akiladevi, S. Sathya, V. Mahalakshmi, and D. A. Kumar, "NeuroAI-Driven Advanced Deep Brain Stimulation for Precision Management of Movement Disorders," 2023 2nd Int. Conf. Autom. Comput. Renew. Syst., pp. 1489–1494, 2023, doi: 10.1109/ICACRS58579.2023.10404966.

[9] M. Mittal, L. M. Goyal, S. Kaur, I. Kaur, A. Verma, and D. Jude Hemanth, "Deep learning based enhanced tumor segmentation approach for MR brain images," Appl. Soft Comput., vol. 78, pp. 346–354, May 2019, doi: 10.1016/j.asoc.2019.02.036.

[10] K. Yamini, K. N. Kumar Reddy, and T. Jaswanth, "Probabilistic GA-NARX based Approach for Brain Tumor Classification Via Tumor Region Partition and Augmentation," Int. Conf. Sustain. Commun. Networks Appl. ICSCNA 2023 - Proc., no. Icscna, pp. 1454–1459, 2023, doi: 10.1109/ICSCNA58489.2023.10370523.

[11] M. Gotz, C. Weber, J. Blocher, B. Stieltjes, H. Meinzer, and K. Maier-Hein, "Extremely randomized trees based brain tumor segmentation. in Proceedings of BRATS Challenge - MICCAI. 2014," Researchgate.Net, no. March 2015, pp. 1–6, 2014, [Online]. Available: http://people.csail.mit.edu/menze/papers/proceedings_miccai_brats_2014.pdf

[12] T. D. Shukla, K. Kalpana, R. Gupta, D. Kalpanadevi, A. A. Walid, and K. K. Kumar, "A Novel Machine Learning Algorithm for Prostate Cancer Image Segmentation using mpMRI," 2023 Int. Conf. Sustain. Comput. Smart Syst., no. Icscss, pp. 96–101, 2023, doi: 10.1109/ICSCSS57650.2023.10169504.

[13] M. P. B, "Integrating Deep Learning and Graph Neural Networks for Multimodal Lung Tumor Analysis : A Novel Approach for Improved Classification and Predict," 2023 Int. Conf. Self Sustain. Artif. Intell. Syst., no. Icssas, pp. 346–352, 2023, doi: 10.1109/ICSSAS57918.2023.10331691.

[14] Z. Cebeci, C. Cebeci, Y. Tahtali, and L. Bayyurt, "Two novel outlier detection approaches based on unsupervised possibilistic and fuzzy clustering," PeerJ Comput. Sci., vol. 8, p. e1060, Sep. 2022, doi: 10.7717/peerj-cs.1060.

[15] G. Sreelakshmi, S. Arivarasan, S. V. G. V. A. Prasad, N. Saikumari, K. V. Kumari, and A. Vidya, "Improving Brain Stroke Diagnosis with SHAP- Enhanced Predictive Models," 2024 Int. Conf. Data Sci. Netw. Secur., pp. 1–6, 2024, doi: 10.1109/ICDSNS62112.2024.10691233.

[16] "Crystal Clean: Brain Tumors MRI Dataset." Accessed: Jan. 06, 2025. [Online]. Available: https://www.kaggle.com/datasets/mohammadhossein77/brain-tumors-dataset

[17] M. O. Khairandish, M. Sharma, V. Jain, J. M. Chatterjee, and N. Z. Jhanjhi, "A Hybrid CNN-SVM Threshold Segmentation Approach for Tumor Detection and Classification of MRI Brain Images," Irbm, vol. 43, no. 4, pp. 290–299, 2022, doi: 10.1016/j.irbm.2021.06.003.

[18] W. Dou, S. Ruan, Y. Chen, D. Bloyet, and J. M. Constans, "A framework of fuzzy information fusion for the segmentation of brain tumor tissues on MR images," Image Vis. Comput., vol. 25, no. 2, pp. 164–171, 2007, doi: 10.1016/j.imavis.2006.01.025.

[19] S. Anantharajan, S. Gunasekaran, T. Subramanian, and V. R, "MRI brain tumor detection using deep learning and machine learning approaches," Meas. Sensors, vol. 31, no. January, p. 101026, 2024, doi: 10.1016/j.measen.2024.101026.

[20] Y. Peng, S. Wang, X. Long, and B. L. Lu, "Discriminative graph regularized extreme learning machine and its application to face recognition," Neurocomputing, vol. 149, no. Part A, pp. 340–353, 2015, doi: 10.1016/j.neucom.2013.12.065.